Electronic Supplementary Material (ESI) for ChemComm.
This journal is © The Royal Society of Chemistry 2020

Supplementary Information

Molecular Layer Deposition of Li-ion Conducting “Lithicone” Solid Electrolytes

Eric Kazyak,[a]‡ Minjeong Shin,[a]‡ William S. LePage,[a] Tae H. Cho,[a] and Neil P. Dasgupta[ab]*

[a] Department of Mechanical Engineering, University of Michigan, Ann Arbor, MI 48109, USA

[b] Department of Materials Science & Engineering, University of Michigan, Ann Arbor, MI 48109, USA

E-mail: ndasgupt@umich.edu

‡ These authors contributed equally to this work.

EXPERIMENTAL METHODS

ALD/MLD Process

The ALD/MLD processes were carried out in a glovebox-integrated Savannah S200 reactor (Ultratech/Cambridge Nanotech, Inc.). Lithicone films were deposited at 135 °C and 175 °C. Lithium *tert*-butoxide (LiO^tBu, 98+%, Strem Chemicals) and ethylene glycol (EG, 99.8%, Sigma Aldrich) were used as the precursors for deposition. The LiO^tBu source was heated to 170 °C and the EG source was heated to 80 °C to maintain sufficient vapor pressure. Precursor vapor was delivered into the manifold via vapor draw (without a bubbler), and transported to the reactor by the Ar carrier gas. Process parameters were determined by saturation test, which was conducted on single-crystal silicon wafers. In the first test, the LiO^tBu pulse time was varied from 1 s to 16 s, with the EG pulse time fixed at 1 s, while in the second test, the EG pulse time was varied from 0.02 s to 4 s, with the LiO^tBu pulse time fixed at 8 s. The saturated precursor purge time was determined similarly. The precursor pulse lengths were 8 s and 1 s for LiO^tBu and EG, respectively. Each precursor pulse was followed by a 90 s purge, where ultra high purity argon (99.999%) was used during the purging steps, with a carrier gas flow rate of 50 sccm. An *in situ* quartz crystal microbalance was used to monitor the film growth. Post-deposition annealing of the lithicone film was performed at 350 °C for 10 min inside an Ar glovebox.

We note that lithicone films are air sensitive, and thus samples were handled in an argon-protected environment unless otherwise stated. For film characterizations where air exposure was unavoidable, an Al_2O_3 ALD film was used, which used as a capping layer to protect the lithicone (Fig. S11). Al_2O_3 was deposited using trimethylaluminum (TMA, 97%, Sigma Aldrich) and H_2O as precursors. Al_2O_3 deposition on lithicone was performed at 135 °C with TMA pulses of 0.1 s and H_2O pulses of 0.05 s at a carrier gas flow rate of 10 sccm, resulting in a growth rate of 1.1 Å per cycle. 100 ALD cycles of an Al_2O_3 film was grown on lithicone and the Al_2O_3 capping layer was effective in protecting the lithicone from degrading when exposed to air (Fig. S11).

Film Characterization

Spectroscopic ellipsometry measurements were performed using a Woollam M-2000 Ellipsometer with a Si (100) substrate, and data were fit with a Cauchy layer on top of the native oxide of the Si. Due to the air sensitivity of the lithicone film, a thin Al_2O_3 capping layer was applied on the lithicone top surface for ellipsometry measurements. The thickness of the lithicone layer was determined by subtracting the Al_2O_3 layer thickness (measured separately) from the total thickness.

AFM measurements were performed using an MFP-3D Origin+ AFM (Asylum Research) inside an Ar glovebox. Imaging was performed in tapping mode with AC160TS-R3 probes (Asylum Research) and drive amplitude of 500 mV. The average roughness values were calculated using Gwyddion software package on an area 1 µm x 1 µm.

SEM analysis was performed using a FEI Helios Nanolab 650 SEM/FIB with a 1 kV accelerating voltage. A Si trench was first cleaned with a Piranha solution to remove surface contaminants. Following 400 deposition cycles of lithicone, the sample was cleaved to expose the cross-section.

XPS measurements were conducted on a Kratos Axis Ultra DLD with a monochromated Al Kα x-ray source. The films were loaded into the XPS chamber through the argon-filled glovebox, enabling measurement without exposing the sample to the ambient environment. Quantification and peak fitting were performed in CasaXPS using Shirley background fitting. Core scans in Fig. 3 are shown for 135 °C film. Due to the limited number of features in the as-deposited spectra, energy calibration was performed by utilizing the consistency between the treatments in Fig. S5. The primary lithicone peaks and the valence spectra in the raw data line up well in the as-deposited and annealed samples. As the annealed sample show an adventitious C-C peak and a clear lithium carbonate peak, all of the spectra were shifted to align these peaks to 284.8 eV and 290.0 eV, respectively. For the annealed sample, the Li 1s core spectra was deconvoluted by using the area of the lithium carbonate feature in the C1s core scan, and the known composition (Li_2CO_3), and sensitivity factors to calculate the corresponding peak area for the lithium carbonate component of the Li 1s. This method works quite well for films with a homogeneous composition with depth, and was consistent within 5-10% of the components areas across the Li 1s, C 1s, and O 1s regions of the lithium carbonate standard sample in Fig. 3.

XRD analysis was performed using a Rigaku SmartLab diffractometer. To minimize sample air/moisture exposure during XRD measurement, the samples were covered with a PEEK film and sealed to prevent air exposure with Kapton tape.

FTIR analysis was performed on a Bruker Alpha II spectrometer using a Platinum-ATR sampling module with ZnSe crystal. The measurements were performed inside a glovebox, to avoid any air exposure. Al foil was used as the substrate and 400 deposition cycles of lithicone was performed.

Electrochemical Characterization

Measurements of the ionic conductivity were performed by depositing MLD films onto interdigitated Pt electrodes (Metrohm dropsens) on glass substrates. The electrode fingers were 5 μm wide and are separated by 5 μm. This structure amplifies the measured signal and eliminates the need to deposit top-contacts after film deposition. The contact pads were exposed after film deposition using 2000-grit sandpaper, and were contacted with tungsten probes (Signatone) in a custom-built probe station. The temperature of the sample was controlled using a ceramic heater with an integrated thermocouple (Watlow). Potentiostatic electrochemical impedance spectroscopy (EIS) was performed with a 10 mV amplitude and a frequency range of 7 MHz to 10 Hz using a Bio-logic SP-200 potentiostat. Nyquist plots were fit with the equivalent circuit shown in Fig. 4a, using the EC-lab software to extract the resistance associated with ionic

conduction within the film. The ionic conductivity was then calculated using the known geometry of the Pt electrodes and the thickness of the film measured by spectroscopic ellipsometry.

Electronic conductivity was measured for MLD films deposited on interdigitated Pt electrodes. Chronoamperometry was conducted using a Bio-logic SP-200 potentiostat, by applying a constant voltage of 1 V and measuring current as a function of time until the current reached steady state. Electronic conductivity was then calculated using the steady state current density and the thickness of the MLD film.

SUPPLEMENTARY FIGURES

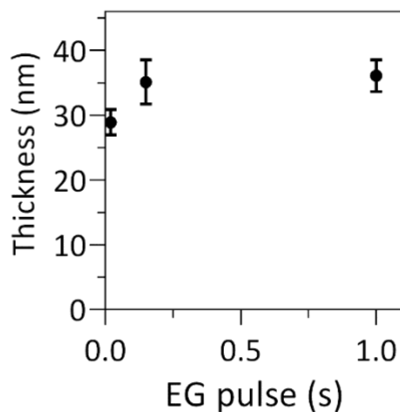

Fig. S1 Thickness of the lithicone film after 200 cycles as a function of EG pulse lengths, focusing on the 0 – 1 s timescale. The thickness reaches plateau at EG pulse of 0.15 s.

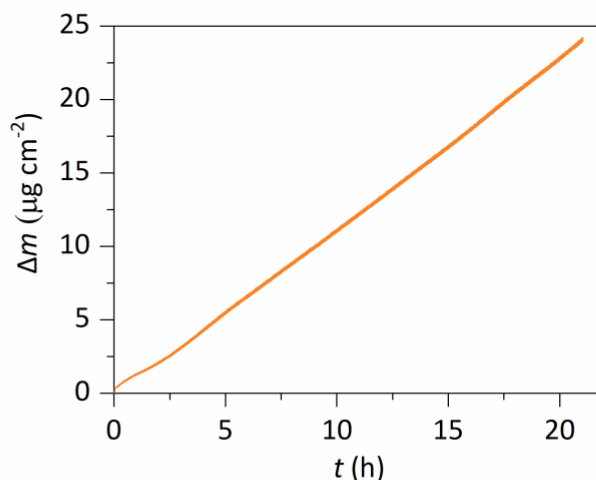

Fig. S2 *In situ* QCM mass gain measured during lithicone film deposition of 400 cycles, showing a linear growth profile.

The initial deposition cycle between 0–2.5 h show a slight deviation from linear growth, suggesting the presence of nucleation delay of lithicone deposition on the QCM substrate (here the lithicone deposition was performed on a QCM that has been previously covered with Al_2O_3). We note that the nucleation delay observed in QCM is different than that seen in ellipsometry measurements (Fig. 1c) and we attribute this to varying nucleation mechanism on different substrates.

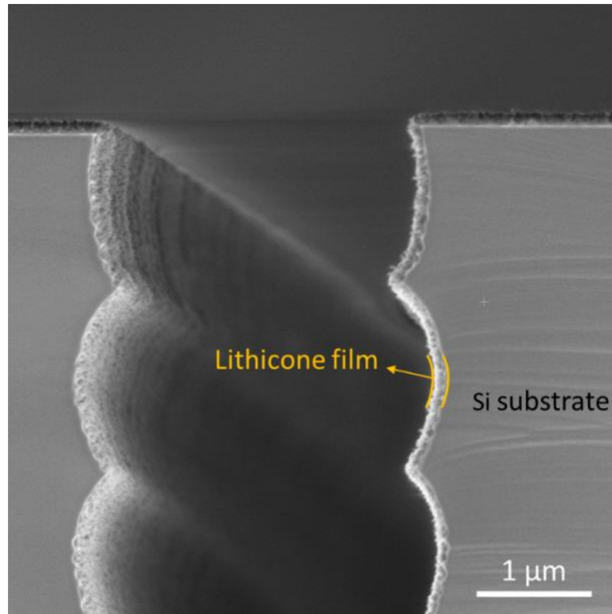

Fig. S3 SEM image of etched Si trench deposited with lithicone film, showing conformal deposition of the lithicone MLD process. The Si trench was prepared by deep reactive ion etching, and the trench in the image has an aspect ratio of 1.54.

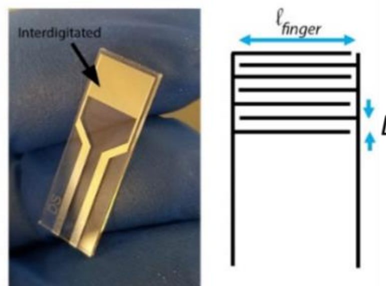

Fig. S4 Schematic of the interdigitated Pt electrode used to measure the ionic conductivity.

The Pt interdigitated electrode has pre-defined distance (*L*) between the two electrodes and the number of fingers. The area of the electrode (*A*) is determined by the equation below, where t_{MLD} is the thickness of the MLD film (determined separately by ellipsometry), l_{finger} is the finger length, and *N* is the number of fingers.

$$A = t_{MLD} \times l_{finger} \times N$$

The resistance (*R*) between the two electrodes is measured and the ionic conductivity (σ) is determined using the following equation.

$$\sigma = \frac{L}{R \times A}$$

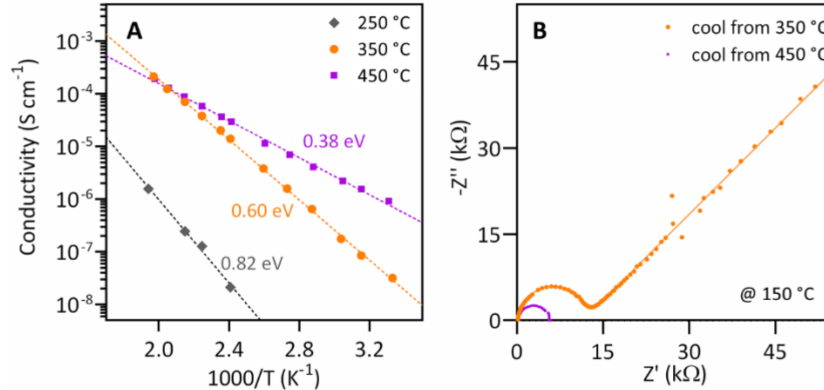

Fig. S5 The effect of annealing temperature on lithicone ionic conductivity is shown. (a) Arrhenius plot of lithicone conductivities of upon heating to 250 °C, 350 °C, and 450 °C, respectively. (b) Nyquist plots of films after post-deposition annealing at 350 °C and 450 °C, respectively, followed by cooling to 150 °C. The Nyquist plots shown are measured at 150 °C.

The variation in ionic conductivity at various annealing temperatures of 250 °C, 350 °C, and 450 °C was studied. Upon annealing upto 350 °C, the ionic conductivity increases with increasing annealing temperature, along with a decrease in activation energy. Under these annealing conditions, the lithicone is primarily an ionic conductor with ionic transference number greater than 0.99999. Upon annealing at higher temperature of 450 °C, the lithicone film becomes a mixed ionic-electronic conductor, showing transference number of ~0.98. This transition to a mixed conductor is also evidenced by the low-frequency tail of the Nyquist plot.

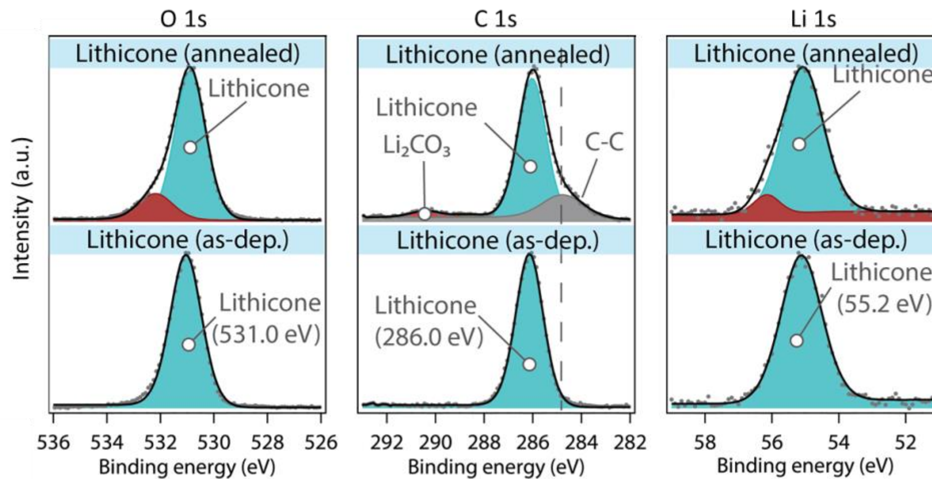

Fig. S6 XPS spectra of the as-deposited lithicone (bottom row) and annealed lithicone (top row). Annealing of the lithicone film was performed at 350 °C for 10 min under argon environment. Upon annealing of the lithicone film, the composition change of the film is negligible (<1.5%). However, we note that the annealed film has higher adventitious carbon and Li_2CO_3 character compared to the as-deposited film. This can be attributed to a change in carbon bonding within

the film or changes in the surface energy after annealing, which impacts the adsorption or carbonaceous species from the gas phase.

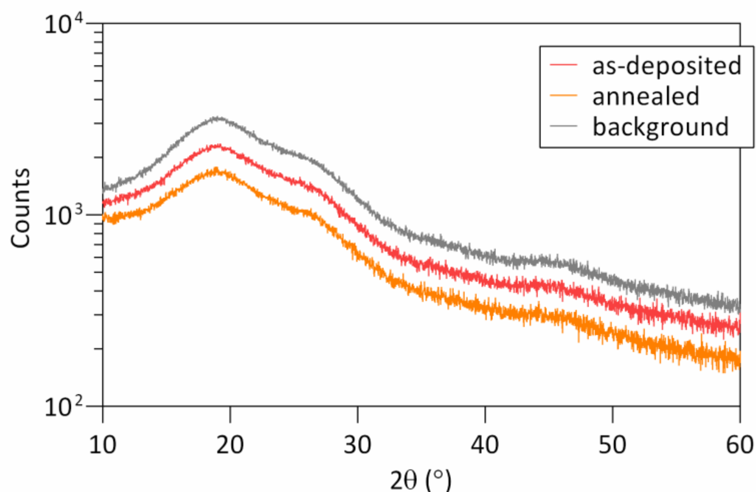

Fig. S7 XRD pattern of as-deposited lithicone and annealed lithicone. The background spectrum (glass slide + PEEK film + Kapton®a tape) without lithicone is also shown for reference. XRD analysis show that the lithicone film remains amorphous after annealing, suggesting no phase transition upon annealing.

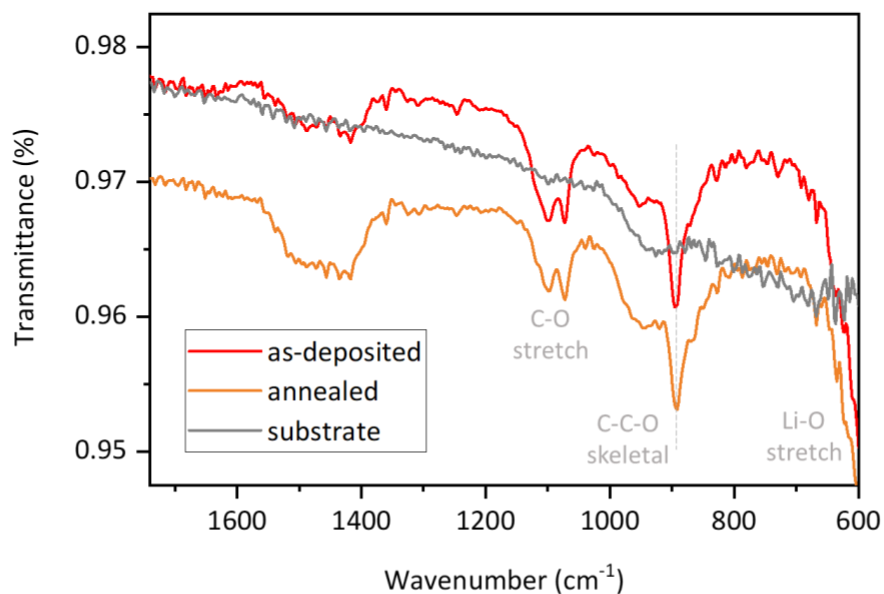

Fig. S8 FTIR spectra of as-deposited lithicone and annealed lithicone. The vibrational modes present in lithicone remain unchanged after annealing. Peak assignments are from Ref. 31.

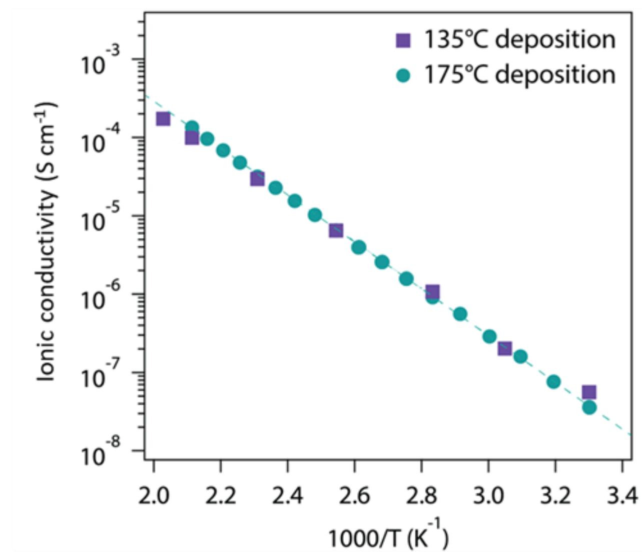

Fig. S9 Arrhenius plot obtained from lithicone films deposited at 135 °C and 175 °C, respectively. The lithicone film deposited at 135 °C and 175 °C shows similar ionic conductivity trend.

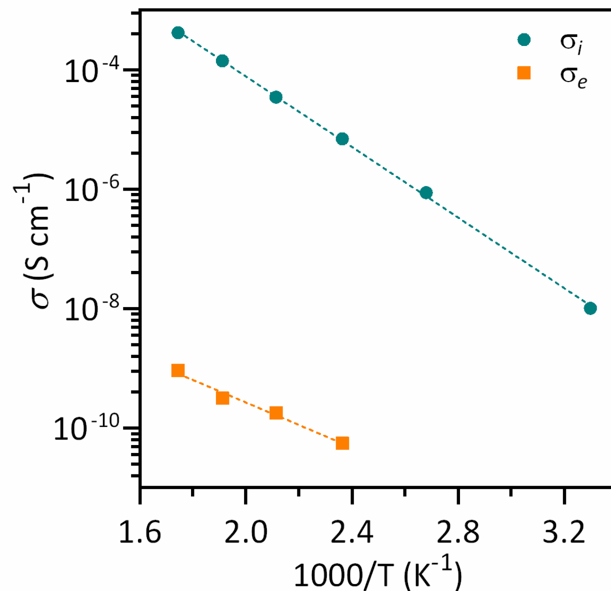

Fig. S10 Arrhenius plot of ionic and electronic conductivities of a lithicone film. Ionic conductivities were measured using EIS and electronic conductivities were measured using chronoamperometry. The ionic transference number at 150 °C was calculated to be 0.999992.

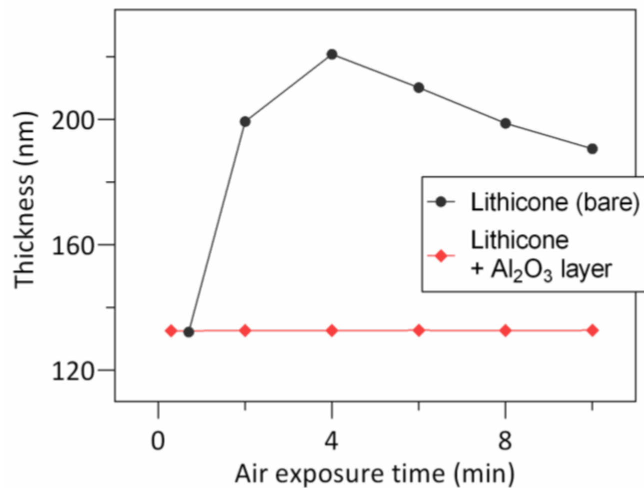

Fig. S11 The thickness of the lithicone films was monitored as a function of air exposure time. Black traces show bare lithicone without a Al_2O_3 capping layer, and red traces show lithicone coated with 11 nm of Al_2O_3 capping layer. The thickness of the bare lithicone film changes significantly when exposed to air, whereas the lithicone with a capping layer shows negligible change in thickness with air exposure.